Ray Optic Approach to Magnetostatic Bulk Wave Propagation in a YIG Film Delay Line

SHANTI S. GUPTA AND NEERAJ C. SRIVASTAVA, MEMBER, IEEE

***Abstract*—This paper discusses a ray optic approach to the magnetostatic wave propagation in a normally magnetized YIG film. The dispersion relation is obtained using the method of transverse resonance. The lateral shift due to reflection at the boundaries has been obtained from energy flow analysis. The path of the rays has been traced from which an approximate expression for the group delay time has been obtained. It is seen that, for the first-order mode, the agreement between this approximate expression for the delay with the rigorous one is satisfactory except near the lower cutoff. In the case of higher order modes, the two compare satisfactorily throughout the frequency range of guided waves.**

I. Introduction

SEVERAL theoretical and experimental investigations have been reported on magnetostatic bulk-wave propagation in layered structures consisting of YIG films and other media [1]–[4]. The main objective of these investigations was their application to microwave signal processing with magnetostatic waves. The analysis [1]–[4] of magnetostatic bulk-wave propagation in YIG films involves the solution of magnetostatic equations subject to appropriate boundary conditions. Such a procedure yields dispersion and delay characteristics but does not provide the necessary physical insight and is difficult to generalize to more complicated configurations.

In recent years, modes in dielectric optical waveguides have been analyzed by zig-zag ray models [5]–[9]. This technique leads to increased physical insight into the nature of guided wave phenomena. Moreover, ray optic methods can be easily generalized to the cases of tapered sections, inhomogeneous and curved guides. An attempt to generalize the zig-zag ray model to guided magnetic waves presents several difficulties. Firstly, unlike in dielectrics, the modes propagating in a ferrimagnetic medium in an arbitrary direction relative to the biasing field, are characterized by complicated dispersion and polarization characteristics. Secondly, since the ferrimagnetics are strongly dissipative and dispersive, all velocities (viz., phase velocity, group velocity, energy velocity, and signal velocity) are, in general, different [10] from one another. Thirdly, since the phase shift on account of total reflection at dielectric–ferrimagnetic interface is a sensitive function of frequency and wavenumber [11], it is difficult to get precise expressions for lateral shift [5], [6], and associated time delay on account of a signal reflection, because it is no longer possible to neglect [12] the second-order and higher derivatives of the phase shift.

In the present paper, the first of these difficulties is solved (in the case of slow magnetic waves) by resorting to magnetostatic analysis. As regards the second difficulty, it has already been shown in an earlier paper [13] that if losses are neglected, the energy velocity (V_e) is equal to the group velocity (V_g) for magnetostatic wave propagation in a normally biased YIG film. Therefore, the knowledge of the path of rays will lead to the energy velocity and hence to the group velocity. Unfortunately, no general solution to the last difficulty is presently available; we have obtained the lateral shift using an approximate method due to Renard [14] and which finally leads only to an approximate expression for group delay.

In Section II, we first consider the reflection of a magnetostatic plane wave at ferrite–dielectric interface. The dispersion relation for guided magnetostatic propagation is derived in Section III, using the method of transverse resonance [8]. In Section IV, the expression for lateral shift is derived using the generalized Renard's analysis [15]. The path of rays is discussed in Section V. The expressions for energy flow velocity and group delay are obtained in Section VI. Finally the results of numerical calculations are discussed in Section VII.

II. Magnetostatic Reflection

The magnetic field $\boldsymbol{h}$ of a magnetostatic wave can be derived from the magnetostatic potential ψ as $\boldsymbol{h}=\nabla\psi$. Assuming magnetization along z-axis and using the conditions $\nabla\cdot\boldsymbol{b}=0$, and $\boldsymbol{b}=\boldsymbol{\mu}\cdot\boldsymbol{h}$, it can be shown that the magnetostatic potential ψ_f in YIG region satisfies the following equation:

$$\left[\mu\left(\frac{\partial^2}{\partial x^2}+\frac{\partial^2}{\partial y^2}\right)+\frac{\partial^2}{\partial z^2}\right]\psi_f=0 \tag{1}$$

where μ is the diagonal element of the permeability tensor $\boldsymbol{\mu}$ for a lossless medium, it is given by

$$\mu=1+\frac{\omega_0\omega_m}{\omega_0^2-\omega^2}$$

$$\omega_0=\gamma H_0 \qquad \omega_m=\gamma(4\pi M_0). \tag{2}$$

The magnetic potential ψ_d in the dielectric region satisfies (1) with μ replaced by unity.

Manuscript received November 19, 1979; revised February 26, 1980. This work was supported by the U.S. National Science Foundation and the University Grants Commission of India.

S. S. Gupta is with the Electro Physics Laboratory, Department of Physics, Indian Institute of Technology, New Delhi-110029, India, on study leave from Ganjdundwara College, Ganjdundwara, Etah, India.

N. C. Srivastava is with the Electro Physics Laboratory, Department of Physics, Indian Institute of Technology, New Delhi-110029, India.

0018-9480/80/0800-0915$00.75 ©1980 IEEE

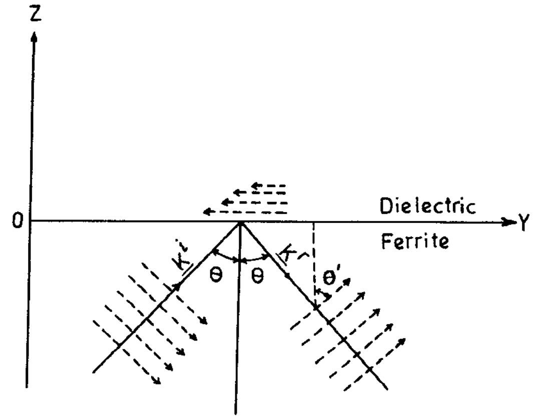

Fig. 1. The total reflection of a magnetostatic plane wave at ferrite–dielectric interface. The broken lines indicate the directions of associated energy flow.

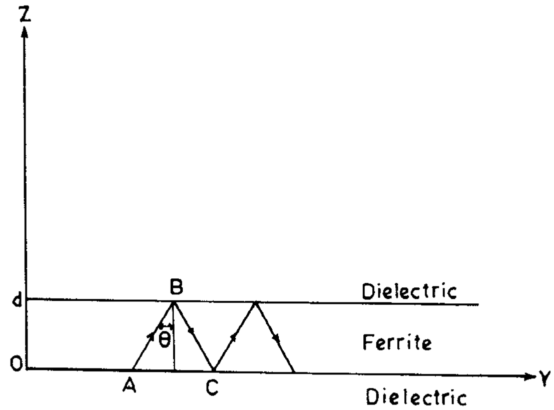

Fig. 2. The phase propagation in a YIG film.

Fig. 1 shows a plane magnetostatic wave which is incident at the YIG–dielectric interface $z=0$. The wave field is uniform along x-axis. If $\boldsymbol{K}^f$ and $\boldsymbol{K}^d$ represent the wave vectors for the incident and transmitted waves, it can be shown from (1) that the magnetostatic field is evanescent in the dielectric region while it is of propagating nature in YIG (for $\mu<0$). Moreover, the components of $\boldsymbol{K}^f$ and $\boldsymbol{K}^d$ can be shown to satisfy the following relations:

$$|K_z^d| = K_y^d$$
$$K_z^f = \alpha K_y^f$$
$$\alpha = \sqrt{-\mu}\,. \tag{3}$$

The angle of incidence of the wave front is given

$$\tan\theta = \frac{K_y^f}{K_z^f} = \frac{1}{\alpha}. \tag{4}$$

The magnetostatic potential for the incident, reflected and transmitted waves is expressed as

$$\psi_i = \exp\left[j\left(\omega t - K_y^f\cdot y - K_z^f\cdot z\right)\right]$$
$$\psi_r = R\exp\left[j\left(\omega t - K_y^f\cdot y + K_z^f\cdot z\right)\right]$$
$$\psi_t = T\exp\left[-|K_z^d|z\right]\exp\left[j\left(\omega t - K_y^d\cdot y\right)\right] \tag{5}$$

where R and T are reflection and transmission coefficients, respectively. The magnetic induction $\boldsymbol{b}$ can be obtained from the magnetostatic potential. The application of appropriate boundary conditions at the interface $z=0$ leads to the following relations:

$$K_y^f = K_y^d (\equiv \beta) \tag{6.a}$$
$$|T| = 2\alpha/\sqrt{1+\alpha^2} \tag{6.b}$$
$$R = \exp(j\phi)$$
$$\phi = 2\arctan(1/\alpha) = 2(m\pi + \theta) \tag{6.c}$$

where $m=0, 1, 2,\cdots$, and ϕ represents the phase shift.

III. Dispersion Relation

The dispersion relation is obtained by generalizing the well known method of transverse resonance [8] to the present case. As shown in Fig. 2, it is required that the phase at points A and C should be the same (or else differ by an integral multiple of 2π which has already been accounted for in (6.c)). Thus, we have

$$2K_z^f\cdot d = 2\phi. \tag{7}$$

Using (3) and (6), this leads to

$$\tan(\alpha\beta d/2) = 1/\alpha \tag{8}$$

which is the same as the dispersion relation obtained from the field analysis [3], [4]. This verifies the applicability of ray optic approach to study magnetostatic wave propagation.

IV. Lateral Shift: Energy Flow Analysis

Under the magnetostatic approximation, the time averaged power flow per unit area and energy density can be expressed as [13]

$$\boldsymbol{P}_{\text{av}} = \text{Re}\left[-\frac{j\omega}{8\pi}\psi^*\boldsymbol{b}\right]$$
$$U_{\text{av}} = \frac{1}{16\pi}\text{Re}\left[\boldsymbol{h}^*\cdot\frac{\partial}{\partial\omega}(\omega\boldsymbol{\mu})\cdot\boldsymbol{h}\right] \tag{9}$$

provided that the losses are neglected. Using (5) and (9) the power flow and energy density are obtained as

$$\boldsymbol{P}^d = \frac{\omega}{8\pi}|T|^2 K_y^d \exp\left(-2|K_z^d|z\right)(-\hat{y})$$
$$U^d = \frac{\left(K_y^d\right)^2}{8\pi}|T|^2\exp\left(-2|K_z^d|z\right). \tag{10}$$

It is noted that, in the dielectric region, the power flow occurs in the negative y direction, i.e., opposite to the direction of phase propagation. This result is consistent with the results of the rigorous field analysis [13]. The direction of energy flow (ray path) in the dielectric region has been shown in Fig. 3. The velocity of energy flow in the dielectric region is obtained as

$$V_e^d = \boldsymbol{P}^d/U^d = (\omega/\beta)(-\hat{y}). \tag{11}$$

Thus the ray optic approach explains the fact that, in the dielectric (or free space) region of an ungrounded YIG film delay line, the magnitudes of the velocity of energy flow [13] is same as the velocity of phase propagation down the guide.

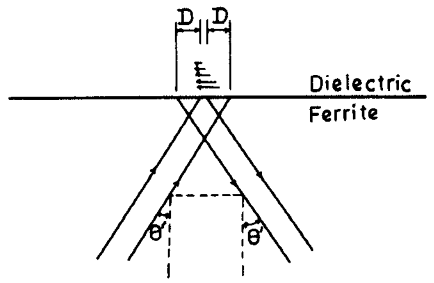

Fig. 3. Illustration of the lateral shift of a reflected ray on account of total reflection. Only energy path is shown.

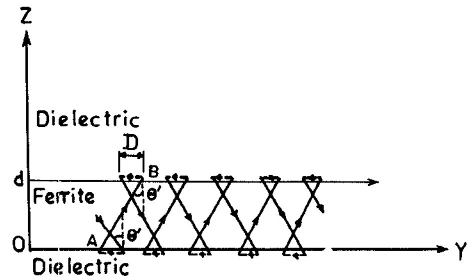

Fig. 4. The path of rays (energy flow) in a YIG film delay line.

Using (9) and (5), the power flow unit area for the incident and reflected waves is obtained as

$$P_i=\frac{\omega\beta}{8\pi}(-\mu\hat{y}-\alpha\hat{z}) \tag{12.a}$$

$$P_r=\frac{\omega\beta}{8\pi}(-\mu\hat{y}+\alpha\hat{z}). \tag{12.b}$$

The energy density is same for the incident and reflected waves and is given by

$$U_{i,r}=\beta^2\omega^2\omega_0\omega_m/\left(8\pi\left(\omega_0^2-\omega^2\right)^2\right). \tag{13}$$

It is easy to show that $K_i\cdot P_i=0=K_r\cdot P_r$, which means that the power flow for incident and reflected plane waves occurs perpendicular to their respective wave vectors; this is explained in Fig. 1. Renard's energy conservation arguments [14], [15] together with (11) lead to the situation which is explained in Fig. 3. Thus the expression for lateral shift on account of total reflection is derived using the Renard's procedure [14], [15] as

$$D=\frac{\int_0^\infty |P_y^d|\,dz}{|P_i|\sin\theta} \tag{14}$$

where D is the lateral shift on total reflection. Referring to Fig. 3 and using (10), (12), and (14), the expression for the lateral shift is obtained as

$$D=\frac{2\sqrt{-\mu}}{\beta(1-\mu)}. \tag{15}$$

V. Path of Rays

A ray represents the path along which energy flows. Since the bulk wave guidance in a YIG film results from multiple internal reflections, it follows from Fig. 3 that the typical path of rays in a YIG film waveguide should be as shown in Fig. 4. Thus the backward propagation of the rays in the dielectric region contributes significantly to large delays. The velocity of energy flow down the film can be obtained from the time required for propagation along the zig-zag ray path of Fig. 4.

VI. Energy Velocity and Time Delay

The time interval τ^d for ray propagation in the dielectric region (in a single reflection), is obtained as

$$\tau^d=\frac{D}{V_e^d}=\frac{2\sqrt{-\mu}}{\omega(1-\mu)}. \tag{16}$$

The speed of energy flow in the YIG region (along the ray path from point A to point B in Fig. 4) is obtained from (12) and (13) as

$$V_e^f=\frac{\sqrt{-\mu(1-\mu)}}{\beta\omega\omega_0\omega_m}\left(\omega_0^2-\omega^2\right)^2. \tag{17}$$

Hence the time delay τ^f in the YIG region is obtained as

$$\tau^f=\frac{x}{V_e^f}=\frac{d\beta\omega\omega_0\omega_m}{\alpha\left(\omega_0^2-\omega^2\right)^2} \tag{18}$$

in which $k=d\sec\theta'=d\operatorname{cosec}\theta$ is the ray path from point A to point B.

Finally, the group delay time per unit distance of propagation is obtained as

$$\tau=\frac{1}{V_e}=\frac{\tau^f+\tau^d}{k\cos\theta-D}. \tag{19}$$

Substitution for x, D, τ^d, and τ^f from (15), (16), and (18) leads to

$$\tau=\frac{\beta\omega\omega_0\omega_m}{\alpha^2\left(\omega_0^2-\omega^2\right)^2}\left[\frac{1+\dfrac{2\alpha^2\left(\omega_0^2-\omega^2\right)^2}{\beta d(1-\mu)\omega^2\omega_0\omega_m}}{1-\dfrac{2}{\beta d(1-\mu)}}\right] \tag{20}$$

which approaches the group delay as obtained from the magnetostatic field analysis [13] in the vicinity of resonance, i.e., when

$$\omega\to\sqrt{\omega_0(\omega_0+\omega_m)}\,.$$

VII. Numerical Results and Discussion

Numerical calculations have been performed in order to investigate the frequency dependence of time delay for the first three modes. The time delay as obtained from the present ray optic approach, i.e., (20) and from field analysis [13] is compared in Fig. 5. In the case of first mode, there is reasonable agreement near the resonance but practically no quantitative or qualitative agreement near the cutoff. This is presumably due to the fact that the expressions for D and τ^d are obtained from approximate analysis. However, for the second and third order modes, there is reasonable agreement over the most of the frequency range of allowed modes; the agreement is, in fact, better near the cutoff.

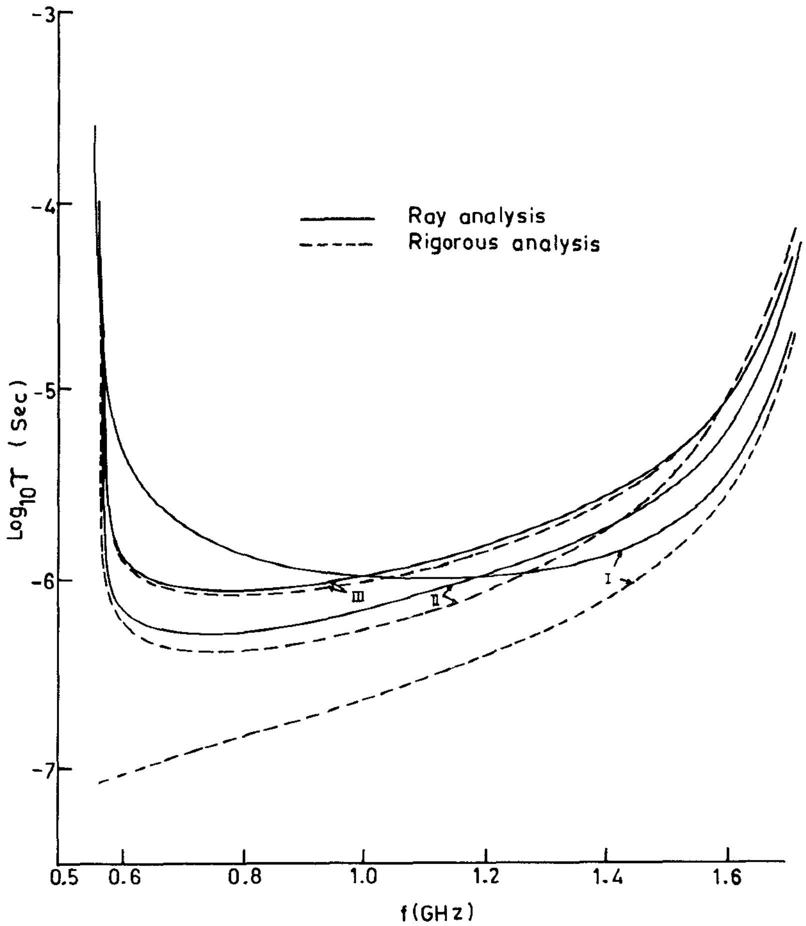

Fig. 5. The comparison of time delay obtained from ray analysis and rigorous analysis for the first three modes. The parameters are $H_0 = 200$ Oe, $(4\pi M_0) = 1750$ Oe, $y = 1.76 \times 10^7$ rad /s·Oe, and $d = 15 \times 10^{-4}$ cm.

VIII. Conclusions

A ray optical approach has been developed to describe the propagation of magnetostatic bulk waves in a normally biased YIG film. The analysis and numerical results lead to the following conclusions.

1) The dispersion relation for magnetostatic propagation in a normally magnetized YIG film is obtained by using the method of transverse resonance; the required phase shift due to total reflection of the wave at the YIG dielectric interface can be obtained within the frame work of magnetostatic analysis.

2) The energy flow in an evanescent field in the dielectric region occurs in a direction opposite to that of phase propagation. The magnitude of the velocity of energy flow is the same as the velocity of phase propagation parallel to the interface. This conclusion is consistant with a rigorous magnetostatic field analysis of the energy distribution and power flow in a YIG film delay line carried out earlier [13] by the authors.

3) The path of rays (i.e., the direction of energy flow, Fig. 4) is different from the path of phase fronts (Fig. 2). Specifically, the circulation of energy back and forth (Fig. 4) seems to be responsible for long delays, compared with dielectric and metallic waveguides.

4) The expression for delay as obtained from the present ray optic approach reduces to the rigorous expression for group delay only in the vicinity of resonance. Although, the numerical results for second ($m = 1$) and higher order modes, as obtained from the two approaches, compare reasonably well throughout the frequency range of allowed modes, the corresponding results for the first order mode (which is, incidently, the dominant mode) show gross disagreement near the cutoff. This is, presumably, due to the approximate nature of the expression for the lateral shift. Therefore, an approach is still to obtain rigorous expressions for the lateral shift and the associated time delay (in a single reflection) for dispersion within the frame work of the ray optic approach.

Acknowledgment

The authors are extremely grateful to Prof. M. S. Sodha and Dr. D. P. Tewari for their kind encouragement and useful suggestions to carry out this work.

References

[1] R. W. Damon and J. R. Eshbach, "Magnetostatic modes of a ferromagnetic slab," *J. Phys. Chem. Solids*, vol. 19, no. 3/4, pp. 308–320, 1961.
[2] J. D. Adam and J. H. Collins, "Microwave magnetostatic delay

devices based on epitaxial yttrium iron garnet," *Proc. IEEE*. vol. 64, no. 5, pp. 794–800, 1976.
[3] N. D. J. Miller, "Magnetostatic volume wave propagation in a dielectric layered structure," *Phys. Stat. Sol. (a)*, vol. 37, pp. 83–91, 1976.
[4] Z. M. Bardai, J. D. Adam, J. H. Collins, and J. P. Parekh, "Delay lines based on magnetostatic volume waves in epitaxial YIG," *AIP Conf. Proc.* no. 34, pp. 268–270, 1976.
[5] N. S. Kapany and J. J. Burke, *Optical Waveguides*. New York, Academic, 1972.
[6] M. S. Sodha, G. D. Gautama, and A. K. Chakravarty, "Propagation of optical pulses through claded fibers: Modified theory," *Appl. Optics*, vol. 12, pp. 2482–2485, 1973.
[7] H. Kogelnik and H. P. Weber, "Rays, stored energy and power flow in dielectric waveguides," *J. Opt. Soc. Amer.*, vol. 64, pp. 174–185, 1974.
[8] P. K. Tien, "Integrated optics and new wave phenomena in optical waveguides," *Rev. Mod. Phys.*, vol. 49, pp. 361–420, 1977.
[9] V. Ramaswamy, "Ray model of energy and power flow in anisotropic film waveguides," *J. Opt. Soc. Amer.*, vol. 64, pp. 1313–1320, 1974.
[10] L. Brillouin, *Wave Propagation and Group Velocity*, New York: Academic, 1960.
[11] N. C. Srivastava, "Non-reciprocal reflection of Electromagnetic waves from magnetized ferrite," *J. Appl. Phys.*, vol. 49, pp. 3181–3189, 1978.
[12] L. M. Brekhoskikh, *Waves in Layered Media*. New York: Academic 1960, p. 104.
[13] S. S. Gupta and N. C. Srivastava, "Power flow and energy distribution of magnetostatic bulk waves in a dielectric layered structure," *J. Appl. Phys.*, 1979.
[14] R. H. Randard, "Total reflection: A new evaluation of the Goos-Hanchen shift," *J. Opt. Soc. Amer.*, vol. 54, pp. 1190–1197, 1964.
[15] S. S. Gupta and N. C. Srivastava, "Physics of microwave reflection at a dielectric-ferrite interface," *Phys. Rev. B*, vol. 19, pp. 5403–5412, 1979.

Surface Electromagnetic Wave Field Strength Measurements on Railroad Tracks

BRIAN C. H. LAI AND CHARLES A. GOBEN, MEMBER, IEEE

***Abstract*—This paper reports an experimental investigation of surface electromagnetic wave (SEW) energy distribution on railroad tracks. Radial field distribution of SEW on 112-lb/yd rails were examined utilizing a dipole diode detector. Laboratory and on site measurements were made. The field strength distribution data at frequencies 3.000, 6.000, and 9.733 GHz show that the main part of the SEW TE mode energy (almost 90 percent) is on the head of the rail. Use of dielectric augmentation on the side of rails resulted in lower attenuation of the propagating SEW. Thick dielectric strip augmentation data shows enhancement of SEW propagation in agreement with McAulay. The intertrack coupling and the characteristic frequency response versus field strength at varied distances from the source were also examined. These data indicate propagation distances of more than 2000 m are possible using dielectric augmentation.**

I. Introduction

OBSTACLE detection and communication for high-speed railroad systems have been playing an increasingly important role in railroad system performance. Automation can contribute to economical operation in such systems. Surface electromagnetic wave (SEW) excitation techniques and their applications have been considered in many papers which involve the United States, United Kingdom, Japan, and Canada. One such microwave communication system for centralized train traffic control utilized the TE_{01} mode propagating within a circular waveguide [1]. The use of guided high-frequency electromagnetic waves transmitted parallel to the railway track for the purpose of providing radar location of trains as well as continuous telephonic communication with drivers and guards on the trains has been developed by the Britich [2]. In Japan, a metallic waveguide with periodic teeth ("Corrugated-Y-Guide") and a radar set have been developed for a moving block system and obstacle detection in high-speed railways [3], [4]. A Sommerfeld Goubau wave propagated on the surface of a G line may also be used for train and obstacle detection [5].

Currently, there is a strong interest in surface electromagnetic waves utilizing several SEW excitation techniques [6]–[9]. One attempt to minimize the vast inventory on the system is to adapt the track for use as an open waveguide [9]. A prism coupler which has no physical contact with the rail was designed in order to excite and detect surface electromagnetic signals from the train. The field patterns are needed to assist in the design of suitable antennas for coupling the appropriate mode in and out of the wave guide in order to utilize the prism coupling technique [8] in an application to collision avoidance [9].

Manuscript received November 4, 1979; revised February 26, 1980. This work was supported in part by the U.S. Department of Transportation under Contracts DOT-TSC-1150-Goben and DOT-TSC-1217-Goben.

B. C. N. Lai was with the Engineering Research Laboratory, University of Missouri-Rolla, Rolla, MO 94070. He is now with the Communications Transistor Corporation, Varian Associates, San Carlos, CA 94070.

C. A. Goben is with the Department of Electrical Engineering and the Engineering Research Laboratory, University of Missouri-Rolla, Rolla, MO 65401.

0018-9480/80/0800-0919$00.75 ©1980 IEEE